

Macroscopic Einstein-Podolsky-Rosen pairs in superconducting circuits

L.F. Wei,^{1,2} Yu-xi Liu,¹ Markus J. Storcz,^{1,3} and Franco Nori^{1,4}

¹Frontier Research System, The Institute of Physical and Chemical Research (RIKEN), Wako-shi, Saitama, 351-0198, Japan

²Institute of Quantum Optics and Quantum Information, Department of Physics, Shanghai Jiaotong University, Shanghai 200030, P.R. China

³Physics Department, ASC, and CeNS, Ludwig-Maximilians-Universität, Theresienstrasse 37, 80333 München, Germany

⁴Center for Theoretical Physics, Physics Department, CSCS, The University of Michigan, Ann Arbor, Michigan 48109-1040, USA

(Dated: February 9, 2020)

We propose an efficient approach to prepare Einstein-Podolsky-Rosen (EPR) pairs in currently-existing Josephson nanocircuits with capacitive-couplings. In these fixed-coupling circuits, two-qubit logic gates could be easily implemented while, strictly speaking, single-qubit gates cannot be easily realized. For a known two-qubit state, conditional single-qubit operations could still be designed to evolve only the selected qubit and keep the other qubit unchanged; the rotations of the selected qubit depends on the state of the left one. These conditional single-qubit operations allow to deterministically generate the well-known Einstein-Podolsky-Rosen pairs, represented by EPR-Bell (or Bell) states, at a macroscopic level. Quantum-state tomography is further proposed to experimentally confirm the generation of these states. The decay of the prepared EPR pairs is analyzed using numerical simulations of the system dynamics. Possible applications of the generated macroscopic EPR pairs to test Bell's Inequality (BI) are also discussed.

PACS number(s): 03.67.Mn, 03.65.Wj, 85.25.Dq.

I. INTRODUCTION

Quantum mechanics (QM) is a very successful theory. It has solved many physical mysteries in both macroscopic superconductivity and microscopic elemental-particle systems. Still, laboratory studies of its conceptual foundations and interpretation continue to attract much attention. One of the most important examples is the well-known Einstein-Podolsky-Rosen (EPR) “paradox”, concerning the completeness of QM. Based on a *gedanken* experiment, Einstein, Podolsky and Rosen (EPR) claimed [1] that QM is incomplete and that so-called “hidden variables” should exist. This is because a two-particle quantum system might be prepared in a correlated state such that a measurement performed on one of the particles immediately changes the state (and thus the possible physical outcome) of the second particle, even though the two particles could be separated by large distances, without direct communication between them. This “paradox” lead to much subsequent, and still on-going, research. Bell proposed [2] an experimentally testable inequality to examine the existence of the hidden variables: if this inequality is ever *not* satisfied, then there are no so-called local “hidden variables” and thus there are quantum non-local correlations. Bell's Inequality (BI) has served as one of the most important witnesses of entanglement, which is a correlated feature of composite quantum systems and takes an important role in future quantum information processing.

During the past decade, a number of interesting experiments [3] using entangled photon pairs have been proposed and carried out to investigate the quantum nature of two-particle entangled states. These experiments showed that BI could be strongly violated, and thus agreed with quantum mechanical predictions. Yet, two essential loopholes have not been strictly closed in these experiments. First, the required EPR pairs were generated in a small subset of all pairs created

in certain spontaneous processes, and thus were not deterministically prepared. Second, besides the problem of detector efficiency, the expected locality could not be strictly satisfied as the individual experimental measurements of two particles were not realistically spacelike separated. Therefore, it is necessary to study two-particle entanglement in different, e.g., massive or macroscopic systems, instead of fast-escaping photons. Theoretical proposals include those with e.g., neutral Kaons [4], Rydberg atoms [5], ballistic electrons in semiconductors [6], and trapped ions [7]. Experimentally, in 1997 two Rydberg atoms had been first entangled to form EPR pairs in a high Q cavity by the exchange of a single photon [8]. Later, by exchanging the quanta of the common vibrational mode, EPR correlations of ultralong lifetime had been generated between a pair of trapped cold ions separated a few micrometers apart [9]. Consequently, experimental violations of BI have been verified with the EPR correlations between the two ions [10] and between an atom and a photon [11].

Recent developments of quantum manipulation in coupled Josephson systems [12, 13] allow to experimentally investigate the quantum correlations between two macroscopic degrees of freedom in a superconducting nano-electronic device [14]. Proposals have been made for producing quantum entanglement between two superconducting qubits, e.g., indirectly coupled by sequentially interacting with a current-biased information bus [15, 16], coupled inductively [17, 18], and coupled via a cavity mode [19]. It has also shown [20] that microwave pulses applied to the gate-voltages can entangle two charge-qubit coupled by a large Josephson junction. By introducing effective single-qubit operations, we have shown [21] that the BI could also be tested even in capacitively-coupled Cooper-pair boxes. The robustness of the scheme proposed there [21] is better suited for weak interbit couplings, e.g., when the ratio of the interbit-coupling energy E_m and the Josephson energy E_J of the qubit is small. Here, for *an arbi-*

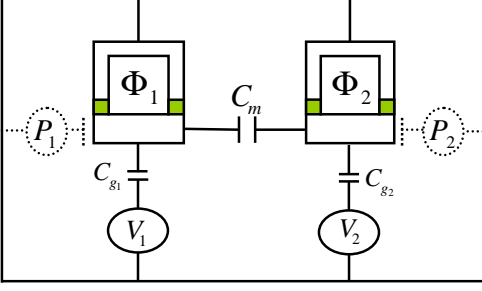


FIG. 1: Two capacitively-coupled SQUID-based charge qubits. The quantum states of two Cooper-pair boxes (i.e., qubits) are manipulated by controlling the applied gate voltages V_1 , V_2 and external magnetic fluxes Φ_1 , Φ_2 (penetrating the SQUID loops). P_1 and P_2 (dashed line parts) read out the final qubit states.

bitrary interbit coupling, we propose an approach for producing EPR correlations by manipulating the well-known EPR-Bell (or Bell) states

$$|\psi_{\pm}\rangle = \frac{1}{\sqrt{2}}(|00\rangle \pm |11\rangle), \quad (1)$$

and

$$|\phi_{\pm}\rangle = \frac{1}{\sqrt{2}}(|01\rangle \pm |10\rangle). \quad (2)$$

The outline of the paper is as follows. In Sec. II, we propose a few elementary quantum operations to deterministically manipulate two superconducting-quantum-interference-device (SQUID)-based Josephson charge qubits coupled capacitively. We show that conditional operations on any selected qubit, keeping the state of the other qubit unchanged, are still possible in the present constant-coupling circuit. By making use of these operations, in Sec. III, we propose a two-step approach to deterministically generate any EPR pairs from the circuit's ground state $|\psi(0)\rangle = |00\rangle$. Further, we discuss how to experimentally confirm the generation of EPR pairs by using a tomographic technique via various experimentally realizable projected measurements. In Sec. IV, considering the existence of typical voltage-noises and $1/f$ -noise, we numerically analyze the decays of the prepared EPR correlations within the Bloch-Redfield formalism [22]. In Sec. V, we discuss the possibility of testing BI with the generated EPR pairs. Conclusions and discussions are given in Sec. VI.

II. MANIPULATIONS OF TWO CAPACITIVELY-COUPLED JOSEPHSON CHARGE QUBITS

We consider the two-qubit nano-circuit sketched in Fig. 1, which was used in recent experiments [12, 23]. Two superconducting-quantum-interference-device (SQUID) loops with controllable Josephson energies produce two

Josephson qubits, fabricated separately (e.g., up to a few micrometers [12, 23]) and coupled via the capacitance C_m . The qubits work in the charge regime with $k_B T \ll E_J^{(j)} \ll E_C^{(j)} \ll \Delta$ (with $j = 1, 2$), wherein both quasi-particle tunnelling and excitations are effectively suppressed and the number n_j (with $n_j = 0, 1, 2, \dots$) of Cooper-pairs in the boxes is a good quantum number. Here, k_B , T , Δ , $E_C^{(j)}$, and $E_J^{(j)}$ are the Boltzmann constant, temperature, superconducting gap, the charging and Josephson energies of the j th qubit, respectively.

Following Refs. [12, 23], the dynamics of the system can be effectively restricted to the subspace spanned by only the four lowest charge states: $|00\rangle$, $|10\rangle$, $|01\rangle$ and $|11\rangle$, and is thus described by the following simplified Hamiltonian

$$\hat{H} = \sum_{j=1,2} \frac{1}{2} \left[E_C^{(j)} \sigma_z^{(j)} - E_J^{(j)} \sigma_x^{(j)} \right] + E_{12} \sigma_z^{(1)} \sigma_z^{(2)}, \quad (3)$$

with $E_{12} = E_m/4$, $E_m = 4e^2 C_m / C_{\Sigma}$, $E_J^{(j)} = 2\varepsilon_J^{(j)} \cos(\pi\Phi_j/\Phi_0)$, and $E_C^{(j)} = E_{C_j}(n_{g_j} - 1/2) + E_m(n_{g_k}/2 - 1/4)$, $j \neq k = 1, 2$ being the coupling-, Josephson- and charge energies, respectively. Here, $n_{g_j} = C_{g_j} V_j / (2e)$, $E_{C_j} = 4e^2 C_{\Sigma_k} / C_{\Sigma}$, and $C_{\Sigma} = C_{\Sigma_1} C_{\Sigma_2} - C_m^2$. Above, e is the electron charge and Φ_0 the flux quantum. $\varepsilon_J^{(j)}$ and C_{Σ_j} are the Josephson energy of the single-junction and the sum of all capacitances connected to the j th box, respectively. The pseudospin operators are defined as $\sigma_z = |0\rangle\langle 0| - |1\rangle\langle 1|$ and $\sigma_x = |0\rangle\langle 1| + |1\rangle\langle 0|$.

Obviously, the interbit-coupling energy $E_{12} = E_m/4$ is determined by the coupling capacitance C_m and therefore given by fabrication and fixed, i.e., not controllable. However, the charge- and Josephson energies of the qubits, $E_C^{(j)}$ and $E_J^{(j)}$, can be controlled by adjusting the applied gate-voltages V_j and fluxes Φ_j . Although any evolution of this two-qubit system is solvable, we prefer certain relatively simple quantum operations for conveniently engineering arbitrary quantum states. These operations can be achieved by properly setting the above controllable parameters.

First, one can switch off all the charge- and Josephson energies and let the circuit evolve under the Hamiltonian $\hat{H}_{\text{int}} = E_{12} \sigma_z^{(1)} \sigma_z^{(2)}$, i.e., undergo a free time-evolution

$$\hat{U}_0(\tau) = \exp \left[-i \frac{E_{12} \tau}{\hbar} \sigma_z^{(1)} \sigma_z^{(2)} \right], \quad (4)$$

in the operational delay τ . We assume the circuit stays in this parameter setting, until any operation is applied to it. In this case, the Bell states Eqs. (1) and (2) will not evolve, once they have been generated.

Second, if $n_{g_1} = n_{g_2} = 1/2$ (co-resonance point) and $E_J^{(1)} = E_J^{(2)} = E_J$, then the circuit has the Hamiltonian $\hat{H}_{\text{co}} = -E_J(\sigma_x^{(1)} + \sigma_x^{(2)})/2 + E_{12} \sigma_z^{(1)} \sigma_z^{(2)}$, which corresponds to the following compact time-evolution operator

$$\bar{U}_{\text{co}} = \frac{1}{2} \begin{pmatrix} a & b & b & c \\ b & a^* & c^* & b \\ b & c^* & a^* & b \\ c & b & b & a \end{pmatrix},$$

with $a = \cos(t\Omega/\hbar) - iE_{12} \sin(t\Omega/\hbar)/\Omega + \exp(-itE_{12}/\hbar)$, $b = iE_J \sin(t\Omega/\hbar)/\Omega$, $c = \cos(t\Omega/\hbar) - iE_{12} \sin(t\Omega/\hbar)/\Omega - \exp(-itE_{12}/\hbar)$, and $\Omega = \sqrt{E_J^2 + E_{12}^2}$. The sub-index ‘‘co’’ refers to ‘‘co-resonance’’. Thus, we can simultaneously flip the two qubits, i.e., $|00\rangle \rightleftharpoons |11\rangle$, and $|01\rangle \rightleftharpoons |10\rangle$, by setting the duration as $\cos(t\Omega/\hbar) = -\cos(tE_{12}/\hbar) = 1$. Another specific two-qubit quantum operation

$$\hat{U}_{\text{co}} = \frac{1}{2} \begin{pmatrix} 1-i & 0 & 0 & 1+i \\ 0 & 1+i & 1-i & 0 \\ 0 & 1-i & 1+i & 0 \\ 1+i & 0 & 0 & 1-i \end{pmatrix} \quad (5)$$

can also be implemented, if the duration is set as $\cos(t\Omega/\hbar) = \sin(tE_{12}/\hbar) = 1$.

Note that a single-qubit logic gate cannot be strictly achieved in the system with strong constant interbit-coupling. Considering the correction of the constant-coupling, we have proposed an effective approach to approximately implement expected single-qubit logic operations [21]. Below, we want to manipulate only one qubit and leave the other one unaffected. Various conditional single-qubit quantum operations (thus, no strict single-qubit quantum logic gates) will be designed to evolve one selected qubit, depending on the state of the other one.

If we switch off all charge energies and one of the Josephson energies, e.g., $E_J^{(2)} = 0$, this will typically yield a Hamiltonian $\hat{H}_J^{(1)} = -E_J^{(1)}\sigma_x^{(1)}/2 + E_{12}\sigma_z^{(1)}\sigma_z^{(2)}$. In this case the circuit undergoes the time evolution

$$\bar{U}_J^{(1)} = \begin{pmatrix} \zeta_1 & \xi_1 & 0 & 0 \\ \xi_1 & \zeta_1^* & 0 & 0 \\ 0 & 0 & \zeta_1^* & \xi_1 \\ 0 & 0 & \xi_1 & \zeta_1 \end{pmatrix},$$

with

$$\begin{aligned} \xi_1 &= i \sin \alpha_1 \sin \left(\frac{t\gamma_1}{\hbar} \right), \quad \cos \alpha_1 = \frac{E_{12}}{\gamma_1}, \\ \zeta_1 &= \cos \left(\frac{t\gamma_1}{\hbar} \right) - i \cos \alpha_1 \sin \left(\frac{t\gamma_1}{\hbar} \right), \\ \gamma_1 &= \frac{1}{2} \sqrt{(2E_{12})^2 + (E_J^{(1)})^2}. \end{aligned}$$

This implies that there are two invariant subspaces $\{|00\rangle, |10\rangle\}$ and $\{|01\rangle, |11\rangle\}$ for this conditional dynamics; the evolution of the first qubit depends on the state of the second qubit, although the later one is unchanged during the dynamics. This operation reduces to

$$\hat{U}_J^{(1)} = \frac{i}{\sqrt{2}} \begin{pmatrix} -1 & 1 & 0 & 0 \\ 1 & 1 & 0 & 0 \\ 0 & 0 & 1 & 1 \\ 0 & 0 & 1 & -1 \end{pmatrix}, \quad (6)$$

if the Josephson energy is set beforehand to $E_J^{(1)} = 2E_{12}$ and the duration is set to satisfy the condition $\sin(\gamma_1 t/\hbar) = 1$.

Similarly, the conditional quantum evolution of the second qubit, keeping the first qubit unchanged, can be implemented

by only switching on the Josephson energy of the second qubit. For example, if $E_J^{(2)} = 2E_{12}$ is set beforehand and the duration satisfies the condition $\sin(\gamma_2 t/\hbar) = 1$, $\gamma_2 = E_{12}\sqrt{2}$, then

$$\hat{U}_J^{(2)} = \frac{i}{\sqrt{2}} \begin{pmatrix} -1 & 0 & 1 & 0 \\ 0 & 1 & 0 & 1 \\ 1 & 0 & 1 & 0 \\ 0 & 1 & 0 & -1 \end{pmatrix}, \quad (7)$$

can be obtained.

The above conditional manipulations on a selected qubit can be further engineered by introducing other controllable parameters, e.g., switching on the charging energies of qubits. In fact, under the Hamiltonian $\hat{H}_{CJ}^{(1)} = E_C^{(1)}\sigma_z^{(1)}/2 - E_J^{(1)}\sigma_x^{(1)}/2 + E_{12}\sigma_z^{(1)}\sigma_z^{(2)}$, the circuit undergoes a time-evolution

$$\bar{U}_{CJ}^{(1)} = \begin{pmatrix} \mu_+ & \nu_+ & 0 & 0 \\ \nu_+ & \mu_+^* & 0 & 0 \\ 0 & 0 & \mu_- & \nu_- \\ 0 & 0 & \nu_- & \mu_-^* \end{pmatrix},$$

with

$$\begin{aligned} \mu_{\pm} &= \cos \left(\frac{t\gamma_{\pm}}{\hbar} \right) - i \cos \alpha_{\pm} \sin \left(\frac{t\gamma_{\pm}}{\hbar} \right), \\ \nu_{\pm} &= i \sin \alpha_{\pm} \sin \left(\frac{t\gamma_{\pm}}{\hbar} \right), \quad \sin \alpha_{\pm} = \frac{E_J^{(1)}}{2\gamma_{\pm}}, \\ \gamma_{\pm} &= \frac{1}{2} \sqrt{[E_C^{(1)}/2 \pm 2E_{12}]^2 + [E_J^{(1)}]^2}. \end{aligned}$$

If the charge energy of the first qubit is beforehand set as $E_C^{(1)} = 2E_{12}$ (thus $\cos \alpha_- = 0$), and the duration is set as $\cos(t\gamma_+/ \hbar) = 1$, then the following two-qubit Deutsch gate [24]

$$\hat{U}_+^{(1)}(\theta_1) = \begin{pmatrix} 1 & 0 & 0 & 0 \\ 0 & 1 & 0 & 0 \\ 0 & 0 & \cos \theta_1 & i \sin \theta_1 \\ 0 & 0 & i \sin \theta_1 & \cos \theta_1 \end{pmatrix}, \quad \theta_1 = \frac{tE_J^{(1)}}{2\hbar}, \quad (8)$$

is obtained. This gate implies that the target qubit (here it is the second one) undergoes a quantum evolution only if the control qubit (here, the first qubit) is in the logical state ‘‘1’’. If the duration is set to simultaneously satisfy the two conditions: $\sin \theta_1 = 1$ and $\cos(t\gamma_+/ \hbar) = 1$, then the above two-qubit operation is equivalent to the well-known controlled-NOT (CNOT) gate, apart from a phase factor. Obviously, if the charge energy of the first qubit is set beforehand as $E_C^{(1)} = -2E_{12}$, then the target qubit undergoes the same evolution only if the control qubit is in the logic state ‘‘0’’, i.e.,

$$\hat{U}_-^{(1)}(\theta_1) = \begin{pmatrix} \cos \theta_1 & i \sin \theta_1 & 0 & 0 \\ i \sin \theta_1 & \cos \theta_1 & 0 & 0 \\ 0 & 0 & 1 & 0 \\ 0 & 0 & 0 & 1 \end{pmatrix}. \quad (9)$$

Note that, due to the presence of the constant interbit-coupling E_{12} , the charge energy $E_C^{(1)}$ depends on both gate-voltages applied to the two Cooper-pair boxes. Switching

off the charge energy $E_C^{(2)} = 0$ requires that the two gate-voltages should be set to satisfy $(n_{g_2} - 1/2)/(n_{g_1} - 1/2) = -2E_{12}/E_{C_2}$. Under this condition the charge energy $E_C^{(1)}$ could still be controlled by adjusting either V_1 or V_2 .

III. MACROSCOPIC EPR-CORRELATIONS: DETERMINISTIC GENERATIONS AND TOMOGRAPHIC CONFIRMATIONS

Now, it will be shown how to deterministically generate EPR correlations between the above two capacitively-coupled Josephson qubits. Then, we propose an effective approach, which is experimentally feasible, to confirm the generation of the EPR states by using tomographic techniques in the present fixed-coupling system. Naturally, we begin with the ground state of the circuit $|\psi(0)\rangle = |00\rangle$, which can be easily initialized by letting the circuit work far from the co-resonance point via a large voltage bias.

First, we superpose two logical states of a selected qubit, e.g., the first one. This can be achieved by simply using a pulse of duration t_1 to implement the above quantum operation (9), i.e.,

$$|\psi_0\rangle \xrightarrow{\hat{U}_-^{(1)}(\theta_1)} |\psi_1\rangle = \frac{1}{\sqrt{2}}(|00\rangle \pm i|10\rangle). \quad (10)$$

Here, the plus sign corresponds to the time durations for $\theta_1 = E_J^{(1)}t_1/(2\hbar) = \pi/4$, and $5\pi/4$. The minus sign corresponds to $\theta_1 = E_J^{(1)}t_1/(2\hbar) = -\pi/4$, and $7\pi/4$.

We next conditionally flip the second qubit, keeping the first one unchanged. The expected operations can be simply expressed as either $|00\rangle \rightarrow |01\rangle$, keeping $|10\rangle$ unchanged, or $|10\rangle \rightarrow |11\rangle$, keeping $|00\rangle$ unchanged. The former (latter) operation requires to flip the second qubit if and only if the first qubit is in logic state ‘‘0’’ (‘‘1’’). These manipulations can be achieved by evolving the circuit under the Hamiltonian $\hat{H}_{CJ}^{(2)} = E_C^{(2)}\sigma_z^{(2)}/2 - E_J^{(2)}\sigma_x^{(2)}/2 + E_{12}\sigma_z^{(1)}\sigma_z^{(2)}$. When the charging energy $E_C^{(2)}$ is set beforehand to $E_C^{(2)} = -2E_{12}$, two of the Bell states can be deterministically created as follows

$$|\psi_1\rangle \xrightarrow{\hat{U}_-^{(2)}(\theta_2)} |\phi_{\pm}\rangle = \frac{1}{\sqrt{2}}(|01\rangle \pm |10\rangle), \quad (11)$$

by accurately setting the duration t_2 of the manipulation

$$\hat{U}_-^{(2)}(\theta_2) = \begin{pmatrix} \cos\theta_2 & 0 & i\sin\theta_2 & 0 \\ 0 & 1 & 0 & 0 \\ i\sin\theta_2 & 0 & \cos\theta_2 & 0 \\ 0 & 0 & 0 & 1 \end{pmatrix} \quad (12)$$

to simultaneously satisfy the conditions $\sin\theta_2 = 1$ and $\cos(\gamma't_2/\hbar) = 1$. Here, $\theta_2 = E_J^{(2)}t_2/(2\hbar)$, and $\gamma' = \sqrt{(E_C^{(2)})^2 + (E_J^{(2)}/2)^2}$. Inversely, by setting $E_C^{(2)} = 2E_{12}$ beforehand, the other two Bell states can be produced as

$$|\psi_1\rangle \xrightarrow{\hat{U}_+^{(2)}(\theta_2)} |\psi_{\pm}\rangle = \frac{1}{\sqrt{2}}(|00\rangle \pm |11\rangle), \quad (13)$$

by using the single-step operation

$$\hat{U}_+^{(2)}(\theta_2) = \begin{pmatrix} 1 & 0 & 0 & 0 \\ 0 & \cos\theta_2 & 0 & i\sin\theta_2 \\ 0 & 0 & 1 & 0 \\ 0 & i\sin\theta_2 & 0 & \cos\theta_2 \end{pmatrix} \quad (14)$$

of the duration satisfying the conditions $\sin\theta_2 = -1$ and $\cos(\gamma't_2/\hbar) = 1$.

The fidelity of these EPR correlations can be experimentally measured by quantum-state tomography, i.e., reconstructing the density matrix of the prepared quantum state. From this reconstructed density matrix, relevant quantum information quantities, such as the degree of entanglement and entropy, can be calculated. For the complete characterization of an unknown two-qubit state with a 4×4 density matrix $\rho = (\rho_{ij,kl})$ (with $i, j, k, l = 0, 1$), we need to determine 15 independent real parameters, due to $\text{tr}\rho = \sum_{i,j=0,1} \rho_{ij,ij} = 1$, and $\rho_{ij,kl} = \rho_{kl,ij}^*$. This can be achieved by a series of measurements on a sufficient number of identically prepared copies of the measured quantum state. The operations presented above for the generation of EPR pairs could provide enough copies of any expected EPR pairs to be reconstructed. Experimentally, Bell states of pseudo-spins (e.g., in nuclear magnetic resonance systems [25], two-level trapped cold ions [9], and the photon pairs [26]) have been tomographically reconstructed by only using a series of single-qubit manipulations. Recently, we have proposed a generic approach to tomographically measure solid-state qubits with switchable interactions [27]. Due to the relatively strong interbit-coupling, which is always on in the circuits considered here, specific operations are required to realize the tomographic reconstruction of the EPR pairs generated.

The state of a charge qubit is often read out by capacitively coupling a single-electron transistor (SET) to the measured qubit [28]. The dissipative current $I_c^{(j)}$ flowing through the j th SET, coupled to the j th qubit, is proportional to the probability of a projective-operator measurement $\hat{P}_j = |1_j\rangle\langle 1_j|$ on the state of density matrix ρ , i.e., $I_c^{(j)} = \text{tr}(\rho\hat{P}_j)$. Such a projective measurement is equivalent to the measurement of $\sigma_z^{(j)}$, as $\sigma_z^{(j)} = (\hat{I}_j - \hat{P}_j)/2$ with \hat{I}_j being the unit operator. For the present system one may perform three kinds of projective measurements: i) the P_1 -measurement (with projected operator $\hat{P}_1 \otimes \hat{I}_2$) acting only on the first qubit (independent of the state of the second qubit); ii) the P_2 -measurement (with projected operator $\hat{I}_1 \otimes \hat{P}_2$) operating only on the second qubit (independent of the state of the first qubit); and iii) the P_{12} -measurement (with projected operator $\hat{P}_1 \otimes \hat{P}_2$) simultaneously acting on both Cooper-pair boxes.

All diagonal elements of the density matrix ρ can be directly determined by performing these three kinds of projective measurements on the system. In fact, $\rho_{11,11}$ can be determined by the P_{12} -measurement as

$$\rho_{11,11} \propto I_c^{(12)} = \text{tr}(\rho\hat{P}_1 \otimes \hat{P}_2). \quad (15)$$

Next, $\rho_{10,10}$ could be determined by P_1 -measurement as

$$\rho_{10,10} + \rho_{11,11} \propto I_c^{(1)} = \text{tr}(\rho\hat{P}_1 \otimes \hat{I}_2). \quad (16)$$

Also, we can determine $\rho_{01,01}$ by the P_2 -measurement as

$$\rho_{01,01} + \rho_{11,11} \propto I_c^{(2)} = \text{tr}(\rho \hat{I}_1 \otimes \hat{P}_2). \quad (17)$$

The remaining element $\rho_{00,00}$ could be determined by the normalization condition $\text{tr}\rho = 1$.

The 12 non-diagonal elements which are left, should be transformed to the diagonal positions of new density matrix $\rho' = \hat{W}\rho\hat{W}^\dagger$, by performing a proper quantum operation \hat{W} on the original density matrix ρ . For example, after a quantum manipulation $\hat{U}_J^{(1)}$, evolving the system to $\bar{\rho} = \hat{U}_J^{(1)}\rho\hat{U}_J^{(1)\dagger}$, we can perform the P_{12} -measurement to obtain

$$\begin{aligned} \bar{I}_c^{(12)} &\propto \text{tr}[\bar{\rho} \hat{P}_1 \otimes \hat{P}_2] \\ &= \frac{1}{2}[\rho_{01,01} + \rho_{11,11} - 2\text{Re}(\rho_{01,11})], \end{aligned} \quad (18)$$

for determining $\text{Re}(\rho_{01,11})$; and perform the P_1 -measurement to obtain

$$\bar{I}_c^{(2)} \propto \text{tr}[\bar{\rho} \hat{P}_1 \otimes \hat{I}_2] = \frac{1}{2}[1 + 2\text{Re}(\rho_{00,10} - \rho_{01,11})], \quad (19)$$

for determining $\text{Re}(\rho_{00,10})$. All the remaining 10 off-diagonal elements of ρ can be similarly determined.

Table I summarizes such a procedure for tomographic characterization of an unknown two-qubit state in this fixed-coupling two-qubit system. We need to first apply to ρ the quantum operations listed in the first column of Table I. Afterwards, the projected measurements listed in the second column of Table I must be made. In this way, all the matrix elements of ρ can be determined. Of course, this is not a unique approach for determining all fifteen independent elements of the density matrix. In fact, the expected tomographic reconstruction could also be achieved by only using the \hat{P}_1 - and \hat{P}_2 -measurements, and making the \hat{P}_{12} -measurement unnecessary.

With the density matrix ρ obtained by the above tomographic measurements and comparing to the density matrix of ideal Bell states, e.g.,

$$\rho_{|\psi_\pm\rangle} = \begin{pmatrix} 1 & 0 & 0 & \pm 1 \\ 0 & 0 & 0 & 0 \\ 0 & 0 & 0 & 0 \\ \pm 1 & 0 & 0 & 1 \end{pmatrix}, \quad \rho_{|\phi_\pm\rangle} = \begin{pmatrix} 0 & 0 & 0 & 0 \\ 0 & 1 & \pm 1 & 0 \\ 0 & \pm 1 & 1 & 0 \\ 0 & 0 & 0 & 0 \end{pmatrix},$$

the fidelity of the EPR pairs generated above can be defined as $F_{|\psi_\pm\rangle} = \text{tr}(\rho\rho_{|\psi_\pm\rangle})$ and $F_{|\phi_\pm\rangle} = \text{tr}(\rho\rho_{|\phi_\pm\rangle})$, respectively.

So far, we have shown that macroscopic EPR correlations could be produced between two capacitively-coupled Cooper-pair boxes. Further, these macroscopic entangled states can be characterized by using tomographic techniques via a series of projective measurements. Below, we will numerically estimate the lifetimes of these macroscopic quantum entangled states and discuss their possible application to test Bell's inequality.

TABLE I: Tomographic characterization of an unknown two-qubit state $\rho = (\rho_{ij,kl})$ with $i, j, k, l = 0, 1$ in capacitively-coupled Josephson circuits. Each row of this table requires operating on an identically prepared initial state ρ .

Operations	Measurement	Determining
No	$\hat{P}_1 \otimes \hat{P}_2$	$\rho_{11,11}$
No	$\hat{P}_1 \otimes \hat{I}_2$	$\rho_{10,10}$
No	$\hat{I}_1 \otimes \hat{P}_2$	$\rho_{01,01}$
$\hat{U}_J^{(1)}$	$\hat{P}_1 \otimes \hat{P}_2$	$\text{Re}(\rho_{01,11})$
$\hat{U}_J^{(1)}$	$\hat{P}_1 \otimes \hat{I}_2$	$\text{Re}(\rho_{00,10})$
$\hat{U}_J^{(2)}$	$\hat{P}_1 \otimes \hat{P}_2$	$\text{Re}(\rho_{10,11})$
$\hat{U}_J^{(2)}$	$\hat{I}_1 \otimes \hat{P}_2$	$\text{Re}(\rho_{00,01})$
$\hat{U}_-^{(1)}(\frac{\pi}{4})\hat{U}_+^{(2)}(\frac{\pi}{2})$	$\hat{P}_1 \otimes \hat{I}_2$	$\text{Re}(\rho_{00,11})$
$\hat{U}_+^{(1)}(\frac{\pi}{4})\hat{U}_+^{(2)}(\frac{\pi}{2})$	$\hat{P}_1 \otimes \hat{P}_2$	$\text{Re}(\rho_{01,10})$
$\hat{U}_-^{(1)}(\frac{\pi}{4})$	$\hat{I}_1 \otimes \hat{P}_2$	$\text{Im}(\rho_{00,10})$
$\hat{U}_+^{(1)}(\frac{\pi}{4})$	$\hat{I}_1 \otimes \hat{P}_2$	$\text{Im}(\rho_{01,11})$
$\hat{U}_-^{(2)}(\frac{\pi}{4})$	$\hat{I}_1 \otimes \hat{P}_2$	$\text{Im}(\rho_{00,01})$
$\hat{U}_+^{(2)}(\frac{\pi}{4})$	$\hat{I}_1 \otimes \hat{P}_2$	$\text{Im}(\rho_{10,11})$
\hat{U}_{co}	$\hat{P}_1 \otimes \hat{P}_2$	$\text{Im}(\rho_{00,11})$
\hat{U}_{co}	$\hat{I}_1 \otimes \hat{P}_2$	$\text{Im}(\rho_{01,10})$

IV. DECAY OF MACROSCOPIC EPR PAIRS DUE TO GATE-VOLTAGE NOISE

The EPR pairs generated above are the eigenstates of the idle (i.e., no operations on it) circuit without any charge- and Josephson energies, and thus are long-lived, at least theoretically. Considering the influence of various disturbing perturbations, these pure quantum states will finally decay to the corresponding mixed states. In fact, experimental solid-state circuits are very sensitive to decoherence because of the coupling to the many degrees of freedom of the solid-state environment. However, coherent quantum manipulations on the generated EPR pairs are still possible if their decay times are not too short.

The typical noise sources in Josephson circuits consist of linear fluctuations of the electromagnetic environment (e.g., circuitry and radiation noises) and the low-frequency noise due to fluctuations in various charge/current channels (e.g., the background charge and critical current fluctuations). Usually, the former one behaves as Ohmic dissipation [29] and the latter one produces a $1/f$ spectrum [30], which is still not fully understood in solid-state circuits (see, e.g., [31]). Here, we assume that the decay of the EPR pairs arises from linear environmental noises, i.e., we investigate the fluctuations of the gate voltages applied to the qubits. Moreover, the effect of background charges that cause dephasing are modeled by setting the zero-frequency part of the bath spectral function to a value given by the experimentally obtained [32] dephasing rates for the charge qubit system. The effect of gate-voltage noise on a single charge qubit has been discussed in [29]. We now study two such noises in a capacitively-coupled circuit. Each electromagnetic environment is treated as a quantum

system with many degrees of freedom and modeled by a bath of harmonic oscillators. Furthermore, each of these oscillators is assumed to be weakly coupled to the Cooper-pair boxes.

The Hamiltonian containing the fluctuations of the applied gate voltages can be generally written as

$$\tilde{H} = \hat{H} + \hat{H}_B + \hat{V},$$

with

$$\hat{H}_B = \sum_{j=1,2} \sum_{\omega_j} \left(\hat{a}_{\omega_j}^\dagger \hat{a}_{\omega_j} + \frac{1}{2} \right) \hbar \omega_j, \quad (20)$$

and

$$\hat{V} = \sigma_z^{(1)}(X_1 + \beta X_2) + \sigma_z^{(2)}(X_2 + \gamma X_1), \quad (21)$$

being the Hamiltonians of the two baths and their interactions with the two boxes. Here,

$$X_j = \frac{E_{C_j} C_{g_j}}{4e} \sum_{\omega_j} (g_{\omega_j}^* \hat{a}_{\omega_j}^\dagger + g_{\omega_j} \hat{a}_{\omega_j})$$

with $\hat{a}_{\omega_j}, \hat{a}_{\omega_j}^\dagger$ being the Boson operators of the j th bath, and g_{ω_j} the coupling strength between the oscillator of frequency ω_j and the non-dissipative system. Due to the mutual coupling of the two Cooper pair boxes, there will be crosstalk of the noise affecting each qubit. This is modelled in the spin-boson model with two bosonic baths presented above by the terms with the additional factors β and γ . The amount of this crosstalk is given by the network of capacitances or the corresponding energies only; namely, $\beta = E_m/2E_{C_2}$ and $\gamma = E_m/2E_{C_1}$, and by inserting experimental values one finds that $\beta \approx \gamma \approx 1/10$.

The effects of these noises can be characterized by their power spectra. The spectral density of the voltage noise for Ohmic dissipation can be expressed as

$$J(\omega) = \pi \sum_{\omega_j} |g_{\omega_j}|^2 \delta(\omega - \omega_j) \sim \pi \alpha \hbar \omega. \quad (22)$$

Here, a Drude cutoff with cutoff frequency $\omega_c = 10^4$ GHz, which is well above all relevant frequency scales of the system, is introduced via $J(\omega) = \alpha \hbar \omega \omega_c^2 / (\omega_c^2 + \omega^2)$. Here, α is a dimensionless constant characterizing the strength of the environmental effects. Introducing the impedance, $Z_t(\omega) = 1/[i\omega C_t + Z^{-1}(\omega)]$, the spectral function for these fluctuations could be expressed as $J(\omega) = \omega \text{Re}(Z_t(\omega))$. Here, $Z(\omega) \sim R_V$ is the Ohmic resistor and C_t is the total capacitance connected to the Cooper-pair box.

The well-established Bloch-Redfield formalism [22, 33] provides a systematic way to obtain a generalized master equation for the reduced density matrix of the system, weakly influenced by dissipative environments. A subtle Markov approximation is also made in this theory such that the resulting master equation is local in time. In the regime of weak coupling to the bath and low temperatures, this theory is numerically equivalent to a full non-Markovian path-integral approach [34]. For the present case, a set of master equations

are obtained in the eigenbasis of the unperturbed Hamiltonian [29]

$$\dot{\rho}_{nm} = -i\omega_{nm} \rho_{nm} - \sum_{kl} R_{nmkl} \rho_{kl}, \quad (23)$$

with the Redfield tensor elements R_{nmkl} given by

$$R_{nmkl} = \delta_{\ell m} \sum_r \Gamma_{nr rk}^{(+)} + \delta_{nk} \sum_r \Gamma_{lr rm}^{(-)} - \Gamma_{\ell mnk}^{(-)} - \Gamma_{\ell mnk}^{(+)}, \quad (24)$$

and the rates Γ^{\pm} are given by the Golden Rule expressions

$$\Gamma_{\ell mnk}^{(+)} = \hbar^{-2} \int_0^\infty dt e^{-i\omega_{nk}t} \langle H_{I,\ell m}(t) H_{I,nk}(0) \rangle,$$

$$\Gamma_{\ell mnk}^{(-)} = \hbar^{-2} \int_0^\infty dt e^{-i\omega_{nk}t} \langle H_{I,\ell m}(0) H_{I,nk}(t) \rangle.$$

Here, $H_{I,\ell m}(t)$ is the matrix element of the bath/system coupling term of the Hamiltonian in the interaction picture, and the brackets denote thermal average.

The strength of the dissipative effects is characterized by the dimensionless parameter α . From experimental measurements of the noise properties of the charge qubit system [35], it is found that the strength of the Ohmic noise is given by

$$\alpha = \frac{4e^2 R}{\hbar \pi} \approx 1.8 \cdot 10^{-3}, \quad (25)$$

where $R \approx 6 \Omega$. Thus, current technology gives a noise floor of approximately $\alpha \sim 10^{-3}$, which will be used for the numerical simulations. For visualization of the decay of the Bell states, we compute the concurrence [36], given by

$$C = \max\{0, \sqrt{\lambda_1} - \sqrt{\lambda_2} - \sqrt{\lambda_3} - \sqrt{\lambda_4}\}. \quad (26)$$

Here, the λ_i are the eigenvalues of $\rho \tilde{\rho}$ and $\tilde{\rho} = (\sigma_y^1 \otimes \sigma_y^2) \rho^* (\sigma_y^1 \otimes \sigma_y^2)$. The concurrence is a measure for entanglement and indicates non-locality. The maximally entangled Bell states (i.e., the ideal EPR correlations) yield a value of 1 whereas a fully separable state gives 0. The results of the simulations are shown in Fig. 2, where the time evolution of the concurrence C shows the decays of all Bell states, for temperature set to an experimentally feasible value of 10 mK. Compared to the durations of quantum manipulations (~ 100 ps), the lifetimes of the operationally idle EPR pairs are sufficiently long.

For the case where only the coupling term between the qubits is present and all single-qubit terms in the Hamiltonian are suppressed, Fig. 2(a) shows that the Bell states exponentially decay. In this case, only pure dephasing, i.e., the zero frequency value $J(\omega = 0)$, contributes to overall decoherence rates, as $\hat{H} = \hat{H}_{\text{int}} = E_{12} \sigma_z^{(1)} \sigma_z^{(2)}$ and $[\hat{H}, \hat{V}] = 0$, see Ref. [37]. The results from microscopic calculations of the magnitude of $1/f$ -noise in these structures are incorporated by introducing a peak in the spectral function at zero frequency. The magnitude of this peak is then determined

by the microscopic derivations of the strength of the $1/f$ -noise in the superconducting charge qubits. Namely, here we set the zero frequency contribution, i.e., the dephasing due to the $1/f$ -noise to an experimentally reported value of $\Gamma_\varphi \approx 10^7$ Hz [32]. Note that the individual contributions from different noise sources sum up in the spectral function $J(\omega) = J_f(\omega) + J_{1/f}(\omega)$, which also holds at $\omega = 0$. It is interesting to note that the decay time is independent of the inter-qubit coupling strength E_{12} . In more detail, when the coupling energy E_{12} in the Hamiltonian is increased the decay does not change. The reason for this behavior is that the pure dephasing is only affected by the zero frequency part of the spectrum, which is obviously independent of the individual frequency splittings, i.e., the characteristic energy scale of the Hamiltonian. Also, one of the most important results from our numerical results (i.e., *the decay time of $|\phi_\pm\rangle$ is longer than that of $|\psi_\pm\rangle$*) is consistent with the analog experimental one in ion traps [9]. This is because $|\phi_\pm\rangle$ is superposed by two states with the same energy, while $|\psi_\pm\rangle$ corresponds to higher energy and is more sensitive to such perturbations.

When the Josephson-tunneling terms exist, e.g., $E_J^{(1)} = E_J^{(2)} = E_J$, we see from Fig. 2(b) that the decays of the generated EPR pairs are significantly faster than in the former case without any tunneling. This is because the additional Josephson tunneling provides additional decoherence channels since the Hamiltonian of the circuit now does not commute with the couplings to the baths. Moreover, also the overall energy scale in the Hamiltonian increases. In this case, the weaker interbit-coupling corresponds to the slower decay of the EPR pairs.

V. TESTING BELL'S INEQUALITY

A possible application of the deterministically generated EPR pairs is to test BI at the macroscopic level. Due to the existence of interbit constant-coupling, the required local operations of encoding classical information $\{\theta_j\}$ into the EPR pairs cannot be strictly implemented. In Ref. [21] we proposed an approach to overcome this difficulty by introducing the effective single-qubit operations including corrections due to the constant-coupling. Instead, here we approximately perform the encoded procedure by sequentially using the conditional single-qubit operations

$$\hat{U}_J^{(1)} = \begin{pmatrix} \vartheta_1 & \chi_1 & 0 & 0 \\ \chi_1 & \vartheta_1^* & 0 & 0 \\ 0 & 0 & \vartheta_1^* & \chi_1 \\ 0 & 0 & \chi_1 & \vartheta_1 \end{pmatrix},$$

and

$$\hat{U}_J^{(2)} = \begin{pmatrix} \vartheta_2 & 0 & \chi_2 & 0 \\ 0 & \vartheta_2^* & 0 & \chi_2 \\ \chi_2 & 0 & \vartheta_2^* & 0 \\ 0 & \chi_2 & 0 & \vartheta_2 \end{pmatrix},$$

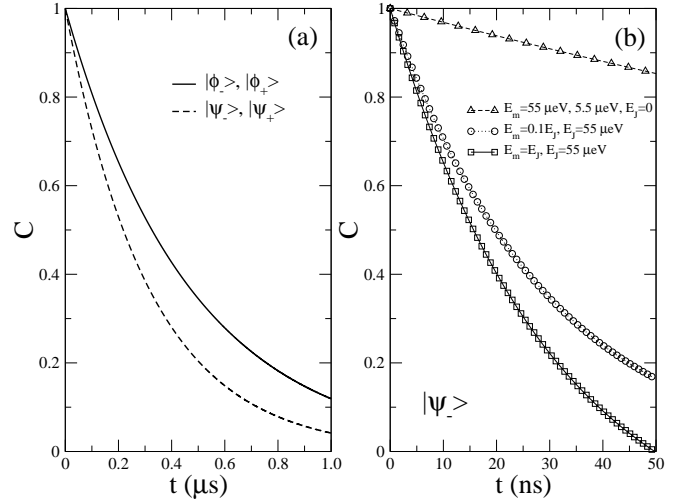


FIG. 2: Simulated time evolution of the concurrence C for a two-qubit system coupled to a noisy environment and initially prepared in the Bell states. Here, the temperature is set to $T = 10$ mK and the strength of the dissipative effects for the two baths is $\alpha^1 = \alpha^2 = 10^{-3}$. (a) captures the long-time decay of the concurrence for different entangled input states in the case of vanishing single-qubit terms, i.e., when only the inter-qubit coupling terms are present. (b) compares the decays of $|\psi_-\rangle$ for different interbit-couplings ($E_m = E_J$, and $0.1E_J$) without ($E_J^{(1)} = E_J^{(2)} = 0$), and with Josephson tunneling ($E_J^{(1)} = E_J^{(2)} = E_J = 55 \mu\text{eV}$).

individually on the two qubits. The operation $\hat{U}_J^{(j)}$ is not a strict single-qubit operation (although it only evolves the j th qubit), as it depends on the state of the k th qubit $j \neq k = 1, 2$. Above, $\chi_j = i \sin \alpha_j \sin \beta_j$, $\vartheta_j = \cos \beta_j - i \cos \alpha_j \sin \beta_j$, $\cos \alpha_j = E_{12}/\gamma_j$, and $\gamma_j = \sqrt{E_{12}^2 + (E_J^{(j)}/2)^2}$, $\beta_j = t\gamma_j/\hbar$. For the case of $\alpha_1 = \alpha_2 = \alpha$, the validity of the above quasi-local encodings could be described by the variation of the degree of entanglement (i.e., *concurrence*) of the EPR pairs

$$\Delta C = 1 - \sqrt{1 - [\sin(2\alpha)(1 - \cos(2\varphi_1 + 2\varphi_2))/2]^2} \quad (27)$$

with $\varphi_j = 2\beta_j$. Obviously, $\Delta C = 0$ corresponds to the ideal locality or maximal locality. After the encoding, we simultaneously detect [13] the populations of qubits and check if they are in the same logic states: the excited one $|1\rangle$ or the ground state $|0\rangle$.

Theoretically, the correlation of two local variables, φ_1 and φ_2 , can be defined as the expectation value of the operator $\hat{P}_T = |11\rangle\langle 11| + |00\rangle\langle 00| - |10\rangle\langle 10| - |01\rangle\langle 01| = \hat{\sigma}_z^{(1)} \otimes \hat{\sigma}_z^{(2)}$ and reads

$$E(\varphi_1, \varphi_2) = \cos^2 \alpha + \sin^2 \alpha \cos(\varphi_1 + \varphi_2). \quad (28)$$

Experimentally, all the above operational steps can be repeated many times in a controllable way for various parameter sets. As a consequence, the correlation function E can be measured by

$$E(\varphi_1, \varphi_2) = \frac{N_{\text{same}}(\varphi_1, \varphi_2) - N_{\text{diff}}(\varphi_1, \varphi_2)}{N_{\text{same}}(\varphi_1, \varphi_2) + N_{\text{diff}}(\varphi_1, \varphi_2)}, \quad (29)$$

TABLE II: Variations of the concurrence, ΔC , correlations E , and CHSH-functions f , for certain typical parameters of the interbit coupling E_m and the controllable classical variables φ_1 and φ_2 .

E_m	(φ_1, φ_2)	ΔC	$E(\varphi_1, \varphi_2)$	f
E_J	$(-\pi/8, -\pi/8)$	0.00699	0.76569	2.6627
	$(-\pi/8, 3\pi/8)$	0.00699	0.76569	
	$(3\pi/8, -\pi/8)$	0.00699	0.76569	
	$(3\pi/8, 3\pi/8)$	0.26943	-0.36569	
$E_J/10$	$(-\pi/8, -\pi/8)$	0.00238	0.72434	2.8264
	$(-\pi/8, 3\pi/8)$	0.00011	0.70784	
	$(3\pi/8, -\pi/8)$	0.00011	0.70784	
	$(3\pi/8, 3\pi/8)$	0.00363	-0.70285	
$E_J/100$	$(-\pi/8, -\pi/8)$	0.00001	0.70711	2.8284
	$(-\pi/8, 3\pi/8)$	0.00001	0.70711	
	$(3\pi/8, -\pi/8)$	0.00001	0.70711	
	$(3\pi/8, 3\pi/8)$	0.00004	-0.70706	

for any pair of chosen classical variables φ_1 and φ_2 . Here, $N_{\text{same}}(\varphi_1, \varphi_2)$ ($N_{\text{diff}}(\varphi_1, \varphi_2)$) are the number of events with two qubits found in the same (different) logic states. With these measured correlation functions, one can experimentally test the BI in macroscopic systems.

We consider the following typical set of angles: $\{\varphi_j, \varphi'_j\} = \{-\pi/8, 3\pi/8\}$ and the interbit couplings $E_m = 4E_{12} = E_J, E_J/10, E_J/100$, respectively. The corresponding variations ΔC of the concurrence and the correlation $E(\varphi_1, \varphi_2)$, which yields the Clauser, Horne, Shimony and Holt (CHSH) [3] function $f = |E(\varphi_1, \varphi_2) + E(\varphi'_1, \varphi_2) + E(\varphi_1, \varphi'_2) - E(\varphi'_1, \varphi'_2)|$, are given in Table II. It is seen that the variations ΔC of the concurrence after the quasi-local operations $\hat{U}_J^{(j)}$, $j = 1, 2$ decrease with decreasing interbit coupling. For very weak coupling, e.g., $E_m/E_J = 0.1$ (or 0.01), the applied conditional single-qubit operations can be regarded as local, away from 0.4%, (or 0.004%). Besides these tiny loopholes of locality, Table II shows that the CHSH-type Bell's inequality [3]

$$f(|\psi'_+\rangle) < 2 \quad (30)$$

is obviously violated.

VI. DISCUSSION AND CONCLUSION

Similar to other theoretical schemes (see, e.g., Ref. [18]) the realizability of the present proposal also faces certain technological challenges, such as the rapid switching of the charge-

and Josephson energies of the SQUID-based qubits and decoherence due to the various environmental noises. Our numerical results, considering various typical fluctuations, showed that the lifetime of the generated EPR pairs adequately allows to perform the required operations for experimentally testing Bell's inequality. Indeed, for current experiments [12], the decay time of a *two*-qubit excited state is as long as ~ 0.6 ns, even for the very strong interbit coupling, e.g., $E_m \simeq E_J$. Longer decoherence times are possible for weaker interbit couplings. In addition, for testing this, the influence of the environmental noises and operational imperfections is not fatal, as the nonlocal correlation $E(\varphi_i, \varphi_j)$ in Bell's inequality is statistical — its fluctuation could be effectively suppressed by the averages of many repeatable experiments.

In summary, for the experimentally demonstrated capacitively-coupled Josephson nanocircuits, we found that several typical two-qubit quantum operations (including simultaneously flipping the two qubits and only evolving a selected qubit in the case of leaving the other one unchanged) could be easily implemented by properly setting the controllable parameters of circuits, e.g., the applied gate voltages and external fluxes. As a consequence of this, macroscopic EPR correlated pairs could be deterministically generated from the ground state $|00\rangle$ by two conditional single-qubit operations; only superposing two logic states of the selected qubit and then only flipping one of the two qubits. During these operations, the left qubit does not evolve. To experimentally confirm the proposed generation schemes, we also propose an effective tomographic technique for determining all density matrix elements of the prepared states by a series of quantum projective measurements. The deterministically generated EPR pairs provide an effective platform to test, at the macroscopic level, certain fundamental principles, e.g., the non-locality of quantum entanglement via violating the Bell's inequality.

The approach proposed here can be easily modified to engineer quantum entanglement in other “fixed-interaction” solid-state systems, e.g., capacitively (inductively) coupled Josephson phase (flux) system and Ising (Heisenberg)-spin chains.

Acknowledgments

We acknowledge useful discussions with Drs. J.Q. You, J.S. Tsai, O. Astafiev, S. Ashhab and F.K. Wilhelm. MJS gratefully acknowledges financial support of RIKEN and the DFG through SFB 631. This work was supported in part by the National Security Agency (NSA) and Advanced Research and Development Activity (ARDA) under Air Force Office of Research (AFOSR) contract number F49620-02-1-0334, and by the National Science Foundation grant No. EIA-0130383.

[1] A. Einstein, B. Podolsky, N. Rosen, Phys. Rev. **41**, 777 (1935).
[2] J. Bell, Phys. **1**, 195 (1964).
[3] See, e.g., G. Weihs, T. Jennewein, C. Simon, H. Weinfurter,

and A. Zeilinger, Phys. Rev. Lett. **81**, 5039 (1998); A. Aspect, J. Dalibard, and G. Roger, *ibid.* **49**, 1804 (1982); W. Tittel, J. Brendel, H. Zbinden, and N. Gisin, *ibid.* **81**, 3563 (1998).

- [4] A. Barmon, Phys. Rev. Lett., **83**, 1 (1999).
- [5] B.J. Oliver and C.R. Stroud, Jr., J. Opt. Soc. Am. B, **4**, 1426 (1987); J.I. Cirac and P. Zoller, Phys. Rev. A **50**, R2799 (1994).
- [6] R. Ionicioiu, P. Zanardi, and F. Rossi, Phys. Rev. A **63**, 050101(R) (2001).
- [7] L.F. Wei and F. Nori, Europhys. Lett. **65**, 1 (2004); L.F. Wei, Yu-xi Liu, and F. Nori, Phys. Rev. A **70**, 063801 (2004); E. Solano, R.L. de Matos Filho, and Z. Zagury, Phys. Rev. A **59**, R2539 (1999).
- [8] E. Hagley, X. Maitre, G. Nogues, C. Wunderlich, M. Brune, J.M. Raimond, and S. Haroche, Phys. Rev. Lett. **79**, 1 (1997).
- [9] C. F. Roos, G. P. T. Lancaster, M. Riebe, H. Häffner, W. Hänsel, S. Gulde, C. Becher, J. Eschner, F. Schmidt-Kaler, and R. Blatt, Phys. Rev. Lett. **92**, 220402 (2004).
- [10] M.A. Rowe, D. Kiepinski, V. Meyer, C.A. Sackett, W.M. Itano, C. Monroe, and D.J. Wineland, Nature **409**, 791 (2001).
- [11] D. L. Moehring, M. J. Madsen, B. B. Blinov, and C. Monroe, Phys. Rev. Lett. **93**, 090410 (2004).
- [12] Yu. P. Pashkin, T. Yamamoto, O. Astafiev, Y. Nakamura, D.V. Averin, and J.S. Tsai, Nature, **421**, 823 (2003).
- [13] R. McDermott, R.W. Simmonds, M. Steffen, K.B. Cooper, K. Cicak, K.D. Osborn, S. Oh, D.P. Pappas, and J.M. Martinis, Science, **307**, 1299 (2005).
- [14] G. P. Berman, A. R. Bishop, D. I. Kamenev, and A. Trombettoni, Phys. Rev. B **71**, 014523 (2005).
- [15] A. Blais, A. M. van den Brink, and A. M. Zagoskin, Phys. Rev. Lett. **90**, 127901 (2003).
- [16] L. F. Wei, Yu-xi Liu, and F. Nori, Europhys. Lett. **67**, 1004 (2004); Phys. Rev. B **71**, 134506 (2005).
- [17] H. Tanaka, Y. Sekine, S. Saito, and H. Takayanagi, Super. Sci. Tech. **14**, 1161 (2001).
- [18] Y. Makhlin, G. Schön, A. Shnirman, Nature **398**, 305 (1999); J.Q. You, S.J. Tsai, and F. Nori, Phys. Rev. Lett. **89**, 197902 (2002).
- [19] J. Q. You and F. Nori Phys. Rev. B **68**, 064509 (2003); G.P. He, S.L. Zhu, Z.D. Wang, and H.Z. Li, Phys. Rev. A **68**, 012315 (2003).
- [20] J. Q. You, J. S. Tsai, and F. Nori, Phys. Rev. B **68**, 024510 (2003).
- [21] L.F. Wei, Yu-xi Liu, and F. Nori, arXiv: quant-ph/0408089; Phys. Rev. B (in press).
- [22] P.N. Argyres and P.L. Kelley, Phys. Rev. **134**, A98 (1964).
- [23] T. Yamamoto, Yu. P. Pashkin, O. Astafiev, Y. Nakamura, and J.S. Tsai, Nature, **425**, 941 (2003).
- [24] A. Barenco, C.H. Bennett, R. Cleve, D.P. DiVincenzo, N. Margolus, P. Shor, T. Sleator, J.A. Smolin, and H. Weinfurter, Phys. Rev. A **52**, 3457 (1995).
- [25] I. L. Chuang, N. Gershenfeld, M. G. Kubinec, and D. Leung, Proc. R. Soc. London, Ser. A **454**, 447 (1998).
- [26] A. G. White, D. F. V. James, W. J. Munro, and P. G. Kwiat, Phys. Rev. A **65**, 012301 (2001); A. G. White, D. F. V. James, P. H. Eberhard, and P. G. Kwiat, Phys. Rev. Lett. **83**, 3103 (1999).
- [27] Yu-xi Liu, L.F. Wei, and F. Nori, Europhys. Lett. **67**, 874 (2004); Phys. Rev. B **72**, 014547 (2005).
- [28] Y. Nakamura, Yu. A. Pashkin and J.S. Tsai, Nature, **398**, 786 (1999).
- [29] U. Weiss, Quantum Dissipative systems, 2nd ed., World Scientific, Singapore, 1999; Y. Makhlin, G. Schön, and A. Shnirman, Rev. Mod. Phys. **73**, 357 (2001).
- [30] A. Shnirman, G. Schön, I. Martin, and Y. Makhlin, Phys. Rev. Lett. **94**, 127002 (2005); E. Paladino, L. Faoro, G. Falci, and R. Fazio, Phys. Rev. Lett. **88**, 228304 (2002).
- [31] H. Gutmann, F.K. Wilhelm, W.M. Kaminsky, S. Lloyd, cond-mat/0308107; G. Falci, A. D'Arrigo, A. Mastellone, E. Paladino, cond-mat/0312442.
- [32] O. Astafiev, private communication (2005).
- [33] M.C. Goorden and F.K. Wilhelm, Phys. Rev. B **68**, 012508 (2003).
- [34] L. Hartmann, I. Goychuk, M. Grifoni, and P. Hänggi, Phys. Rev. E **61**, R4687 (2000).
- [35] O. Astafiev, Yu. A. Pashkin, Y. Nakamura, T. Yamamoto, and J. S. Tsai Phys. Rev. Lett. **93**, 267007 (2004).
- [36] W.K. Wootters, Phys. Rev. Lett. **80**, 2245 (1997).
- [37] M. J. Storcz and F. K. Wilhelm, Phys. Rev. A **67**, 042319 (2003).